

Color Device Calibration: A Mathematical Formulation

Michael J. Vrhel, *Member, IEEE* and H. Joel Trussell, *Fellow, IEEE*

Abstract—The mathematical formulation of calibrating color image reproduction and recording devices is presented. This formulation provides a foundation for future research in areas of characterization of devices and display of color images. The importance of calibration is demonstrated by real examples. The procedure outlined in this paper should become standard for displaying color images for the image processing community.

Index Terms—Color, color calibration, color imaging, color reproduction, colorimetry, printing, scanning.

I. INTRODUCTION

WITH THE advent of low-cost color printers and scanners, there has been increased interest in the image processing community to apply and develop techniques for enhancing, restoring, and reproducing color images [1]. The demonstration of the performance of methods for color image processing has presented a problem due to a variety of reasons. These reasons include an inability to control the final printing process, misunderstandings with regard to color spaces and what RGB really means, and improper or poorly managed scanning to name a few. Problems can be clearly seen in comparing the various “unprocessed” color images of Lena in [1] (a recent special issue on color imaging) with the actual original Lena image. Since the original is not available to most readers, a simulated comparison is shown in Fig. 3, where the commonly used Lena image is (a), which closely matches those shown in [1], and the processed image is (b), which closely matches the original Lena image. The methods used to generate this comparison are the basis of this paper. This example demonstrates the need for a standard image, defined in terms of CIE values, with which to demonstrate color image processing algorithms, in addition to standards for displaying and porting processed images.

In this paper, we explore the problems of achieving control over the color reproduction process. We describe mathematically the process of performing calibrations for scanners, printers etc. This mathematical formulation and its clear and accurate descriptions lay a foundation for future research in this area. In addition, we show how to calibrate a scanner and a printer. This is a necessary process for those in the image

processing community who wish to present results in the area of color image processing.

The paper is organized as follows: in Section II we review notation and color fundamentals. In Sections III–V, we describe the calibration problem for CRT’s, scanners, and printers, respectively. In Section VI, we discuss the problem of gamut mapping. In Section VII, we describe the problem of illumination correction followed by the problem of digital camera calibration in Section VIII. Section IX discusses implementation, Section X presents examples, and finally conclusions are given in Section XI.

II. BACKGROUND

A. Mathematical Notation

We will use a vector space notation for color systems which has proven to be well suited for solving difficult problems in color reproduction [2]–[5]. In the vector notation, the visible spectrum is mathematically uniformly sampled at N wavelengths from about 400 nm to 700 nm [the spectral sensitivity range of the human visual system (HVS)]. An illuminant spectrum $l(\lambda)$ is represented by an N element vector \mathbf{l} and the spectral reflectance of an object is represented by an N element vector \mathbf{r} .

The radiant spectrum reflected from the object with spectral reflectance \mathbf{r} under the illuminant \mathbf{l} can be expressed as \mathbf{Lr} where \mathbf{L} is an $N \times N$ diagonal matrix whose diagonal elements are the elements of the vector \mathbf{l} . The columns of the $N \times 3$ matrix \mathbf{A} contain the sampled CIE XYZ color matching functions and the CIE XYZ value of the spectrum \mathbf{Lr} is given by $\mathbf{t} = \mathbf{A}^T \mathbf{Lr}$.

B. Color Spaces

A *device independent color space* is defined as any space that has a one-to-one mapping onto the CIE XYZ color space. Device independent values describe color for the standard CIE observer. Examples of CIE device independent color spaces include XYZ, Lab, Luv, and Yxy.

By definition, a *device dependent color space* cannot have a one-to-one mapping onto the CIE XYZ color space. In the case of a recording device (e.g., scanners, digital cameras), the device dependent values describe the response of that particular device to color. For a reproduction device (e.g., printers), the device dependent values describe only those colors the device can produce. Thus, for the printer there may exist a one-to-one mapping into the CIE space but not onto it. Note however that for CMYK (four-color) printers,

Manuscript received May 22, 1998; revised March 23, 1999. The associate editor coordinating the review of this manuscript and approving it for publication was Prof. Brian Funt.

M. J. Vrhel is with Color Savvy Systems Limited, Springboro, OH 45066 USA (e-mail: mvrhel@colorsavvy.com).

H. Joel Trussell is with the Department of Electrical and Computer Engineering, North Carolina State University, Raleigh, NC 27695-7911 USA. Publisher Item Identifier S 1057-7149(99)09357-4.

the mappings between in-gamut colors (defined in Section II-C) and the device dependent values are not one-to-one. The CMYK printer can place different ink concentrations on the paper, giving different reflectance spectra, which look the same visually. This effect is defined as *metamerism*.

The use of device dependent descriptions of color presents a problem in the world of networked computers and printers. The same RGB vector can result in different colors on different monitors. Similarly, a specified CMYK value can result in different colors on different printers. Transferring images colorimetrically between multiple monitors and printers with device dependent descriptions is difficult since the user must know the characteristics of the device for which the original image is defined, in addition to the device on which the image is displayed.

An easier method is to define images in terms of a CIE color space and then transform this data to device dependent descriptors for the device on which the image is to be reproduced. The advantage of this approach is that the same image data is easily ported to a variety of devices and there is no need to know the original source of the image. To achieve this ideal situation, it is necessary to determine a function \mathcal{F}_{device} which will provide a mapping from device dependent control values to a CIE color space. If the device is a colorimetric scanner (defined in Section IV), then \mathcal{F}_{device} is sufficient to provide a calibrated device. In the case of a printer, it is necessary to determine a transformation $\mathcal{F}_{device}^{-1}$ (which may or may not exist). Finally, for a monitor, the transformations \mathcal{F}_{device} and $\mathcal{F}_{device}^{-1}$ are both needed since the monitor is used as both a source of image data (e.g., creation of graphics images which are subsequently printed), and as a display device for viewing scanned images.

In the end, the performance of such a methodology is only as good as the relationship of the CIE color space to actual human visual perception. Experiments are still carried out studying perceptual differences and observer variability [6]. Note that as improvements to the CIE color space are made, the mathematics described in this paper will remain valid and just as useful.

C. Device Gamut

Modern printers and display devices are limited in the colors they can produce. This limited set of colors is defined as the *gamut* of the device. If Ω_{cie} is the range of numerical values in the selected CIE color space and Ω_{print} is the numerical range of the device control values, then the set

$$G = \{\mathbf{t} \in \Omega_{cie} | \exists \mathbf{c} \in \Omega_{print} \text{ where } \mathcal{F}_{device}(\mathbf{c}) = \mathbf{t}\} \quad (1)$$

defines the gamut of the color output device. Similarly, the complement set

$$G^c = \{\mathbf{t} \in \Omega_{cie} | \nexists \mathbf{c} \in \Omega_{print} \text{ where } \mathcal{F}_{device}(\mathbf{c}) = \mathbf{t}\} \quad (2)$$

defines colors outside the device gamut. For colors in the gamut, there will exist a mapping between the device dependent control values and the CIE XYZ color space. Colors which are in G^c cannot be reproduced and must be *gamut-mapped* to a color which is within G . The gamut mapping

algorithm \mathcal{D} is a mapping from Ω_{cie} to G , that is $\mathcal{D}(\mathbf{t}) \in G \forall \mathbf{t} \in \Omega_{cie}$.

D. Profiles

A *device profile* is defined by the mappings \mathcal{F}_{device} , $\mathcal{F}_{device}^{-1}$, and \mathcal{D} . These mappings describe the transformation between a CIE color space and the device control values. As mentioned previously, certain devices such as scanners and digital cameras need only have \mathcal{F}_{device} to achieve calibration. In this case, the device profile is defined by that single mapping. The International Color Commission (ICC) has suggested a standard format for describing a profile. This standard profile can be based on a physically-based mathematical model (common for monitors) or a look-up-table (LUT) (common for printers and scanners) [7], [8].

E. Illumination

Typically a device profile is determined for a particular viewing illumination. The viewing illumination is of importance due to the metamerism effect discussed earlier. The importance of illumination is best illustrated by an example.

Consider a printed image that was created via a web offset process. It is desired to print a visual match to this image using a dye sublimation printing process. Let the CIE XYZ value of pixel i in the offset image to be given by

$$\mathbf{t}_{offset_i} = \mathbf{A}^T \mathbf{L}_1 \mathbf{r}_i \quad (3)$$

when the image is under the illuminant \mathbf{L}_1 .

If the dye-sub printer is successfully calibrated, then ignoring gamut mismatches (cf. Section VI)

$$\mathbf{t}_{dyesub_i} = \mathbf{A}^T \mathbf{L}_1 \mathbf{q}_i \quad (4)$$

and

$$\mathbf{A}^T \mathbf{L}_1 \mathbf{q}_i = \mathbf{A}^T \mathbf{L}_1 \mathbf{r}_i. \quad (5)$$

Note that \mathbf{q}_i need not (and rarely will) equal \mathbf{r}_i . For this reason, the images may no longer match when viewed under an illumination \mathbf{L}_2 that is different than \mathbf{L}_1 . As mentioned previously, this effect is defined as metamerism.

To obtain colorimetric matching under multiple illuminants, it is necessary to perform calibration on the spectral level (i.e. $\mathbf{q}_i = \mathbf{r}_i$), which is virtually impossible due to the limited freedom in the printing process (i.e. there are typically only three or four overlaid colorants). High fidelity printing processes that use more than four colorants usually use the additional colorants to increase the size of the gamut rather than attempting to create spectral matches.

Instead of determining a profile for every viewing illumination, it is possible to determine mappings to correct for changes in illumination. The motivation for doing this is that these illumination mappings may be simpler and easier to determine than the highly nonlinear LUT mappings of the device profile. This problem will be discussed after addressing the problems of determining device profiles (cf. Section VII). For the remainder of the paper, the viewing illuminant will be denoted by \mathbf{L}_v .

III. CRTs

A monitor is often used to provide softcopy preview for the printing process. In addition, the monitor is now a common source for user generated images. Monitor calibration is almost always based on a physical model of the device [9]–[12]. A typical model is

$$\begin{aligned} \mathbf{t} &= \mathbf{H}[r', g', b']^T \\ r' &= \left(\frac{r - r_0}{r_{\max} - r_0} \right)^{\gamma_r} \\ g' &= \left(\frac{g - g_0}{g_{\max} - g_0} \right)^{\gamma_g} \\ b' &= \left(\frac{b - b_0}{b_{\max} - b_0} \right)^{\gamma_b} \end{aligned} \quad (6)$$

where \mathbf{t} is the CIE value produced by driving the monitor with control value $\mathbf{d} = [r, g, b]^T$, and the parameters $\gamma_r, \gamma_g, \gamma_b, r_0, g_0, b_0, r_{\max}, g_{\max}, b_{\max}$, and \mathbf{H} are defined in the profile.

Creating a profile for a monitor involves the determination of these parameters where $r_{\max}, g_{\max}, b_{\max}$ are the maximum values of the control values (e.g., 255). To determine the parameters, a series of color patches is displayed on the CRT and measured with a colorimeter which will provide pairs of CIE values $\{\mathbf{t}_k\}$ and control values $\{\mathbf{d}_k\}$ $k = 1, \dots, M$.

Values for $\gamma_r, \gamma_g, \gamma_b, r_0, g_0$, and b_0 are determined such that the elements of $[r', g', b']$ are linear with respect to the elements of XYZ and scaled between the range $[0, 1]$ (cf. (6)) [12]. The matrix \mathbf{H} is then determined from the tristimulus values of the CRT phosphors at maximum luminance. Specifically, the mapping is given by

$$\begin{bmatrix} X \\ Y \\ Z \end{bmatrix} = \begin{bmatrix} X_{R\max} & X_{G\max} & X_{B\max} \\ Y_{R\max} & Y_{G\max} & Y_{B\max} \\ Z_{R\max} & Z_{G\max} & Z_{B\max} \end{bmatrix} \begin{bmatrix} r' \\ g' \\ b' \end{bmatrix} \quad (7)$$

where $[X_{R\max}, Y_{R\max}, Z_{R\max}]^T$ is the CIE XYZ tristimulus value of the red phosphor for control value $\mathbf{d} = [r_{\max}, 0, 0]^T$. The green and blue phosphors are similarly defined. In practice, the CIE XYZ values of the phosphors are mapped to account for perceptual effects and a viewing illumination (cf. Section IX-B).

This standard model is often used to provide an approximation to the mapping $\mathcal{F}_{\text{monitor}}(\mathbf{d}) = \mathbf{t}$. Problems such as spatial variation of the screen or electron gun dependence are typically ignored. A LUT can also be used for the monitor profile in a manner similar to that described below for the scanner calibration.

IV. SCANNERS

Mathematically, the recording process of a scanner can be expressed as

$$\mathbf{z}_i = \mathcal{H}(\mathbf{M}^T \mathbf{r}_i) \quad (8)$$

where the matrix \mathbf{M} contains the spectral sensitivity (including the scanner illuminant) of the three (or more) bands of the device, \mathbf{r}_i is the spectral reflectance at spatial point i , \mathcal{H} models any nonlinearities in the scanner (invertible in the range of

interest), and \mathbf{z}_i is the vector of recorded values. Noise can be treated as in [13], but is not central to the presentation of this paper.

We define *colorimetric scanning* as the process of scanning or recording an image such that the CIE values of the image can be recovered from the recorded data. This means that image reflectances which appear different to a standard observer will be recorded as different device dependent values. Mathematically, this implies

$$\mathbf{A}^T \mathbf{L}_v \mathbf{r}_k \neq \mathbf{A}^T \mathbf{L}_v \mathbf{r}_j \Rightarrow \mathbf{M}^T \mathbf{r}_k \neq \mathbf{M}^T \mathbf{r}_j \quad (9)$$

for all $\mathbf{r}_k, \mathbf{r}_j \in \Omega_r$ $k \neq j$ where Ω_r is the set of physically realizable reflectance spectra. In other words, a colorimetric scanner would “see” the image just as a standard observer under illuminant \mathbf{L}_v .

Given such a scanner, the calibration problem is to determine the continuous mapping $\mathcal{F}_{\text{scan}}$ which will transform the recorded values to a CIE color space. In other words, determine the function $\mathcal{F}_{\text{scan}}$ such that

$$\mathbf{t} = \mathbf{A}^T \mathbf{L}_v \mathbf{r} = \mathcal{F}_{\text{scan}}(\mathbf{z}) \quad (10)$$

for all $\mathbf{r} \in \Omega_r$.

Unfortunately, most scanners and especially desktop scanners are not colorimetric, hence the transformation $\mathcal{F}_{\text{scan}}$ does not exist. This is caused by physical limitations on the scanner illuminants and filters which prevent them from being within a linear transformation of the CIE color matching functions. Work related to designing optimal approximations is found in [14]–[17].

For the noncolorimetric scanner, there will exist spectral reflectances that look different to the standard human observer but when scanned produce the same recorded values. These colors are defined as being metameric to the scanner. Likewise, there will exist spectral reflectances that give different scan values and look the same to the standard human observer. While the latter can be corrected by the transformation $\mathcal{F}_{\text{scan}}$, the former cannot.

On the upside, there will always (except for degenerate cases) exist a set of reflectance spectra over which a transformation from scan values to CIE XYZ values will exist. Printed images, photographs, etc., are all produced with a limited set of colorants. Reflectance spectra from such processes have been well modeled with very few (3–5) principal component vectors [3], [18]–[20]. When limited to such data sets, it may be possible to determine a transformation $\mathcal{F}_{\text{scan}}$ such that

$$\mathbf{t} = \mathbf{A}^T \mathbf{L}_v \mathbf{r} = \mathcal{F}_{\text{scan}}(\mathbf{z}) \quad (11)$$

for all $\mathbf{r} \in B_{\text{scan}}$. In other words, we are restricting ourselves to a set of reflectance spectra B_{scan} over which the continuous mapping $\mathcal{F}_{\text{scan}}$ exists. This idea is also discussed in [21].

LUT’s as well as nonlinear and linear models for $\mathcal{F}_{\text{scan}}$ have been used to calibrate color scanners [22]–[25]. In all of these approaches, the first step is to select a collection of color patches that span the colors of interest. Ideally, these colors should not be metameric in terms of the scanner sensitivities or to the standard observer under the illuminant for which the calibration is being produced. This constraint assures a

one-to-one mapping between the scan values and the device independent values across these samples. In practice, this constraint is easily obtained. The reflectance spectra of these M_q color patches will be denoted by $\{\mathbf{q}\}_k$ for $1 \leq k \leq M_q$.

These patches are measured using a spectrophotometer or a colorimeter which will provide the device independent values

$$\{\mathbf{t}_k = \mathbf{A}^T \mathbf{L}_v \mathbf{q}_k\} \quad \text{for } 1 \leq k \leq M_q. \quad (12)$$

Without loss of generality, $\{\mathbf{t}_k\}$ could represent any colorimetric or device independent values, e.g. CIE Lab, CIE Luv in which case $\{\mathbf{t}_k = \mathcal{L}(\mathbf{A}^T \mathbf{L}_v \mathbf{q}_k)\}$ where $\mathcal{L}(\cdot)$ is the transformation from CIE XYZ to the appropriate color space. The patches are also measured with the scanner to be calibrated providing $\{\mathbf{z}_k = \mathcal{H}(\mathbf{M}^T \mathbf{q}_k)\}$ for $1 \leq k \leq M_q$.

Mathematically, the calibration problem is: find a transformation \mathcal{F}_{scan} where

$$\mathcal{F}_{scan} = \arg \left(\min_{\mathcal{F}} \sum_{i=1}^{M_q} \|\mathcal{F}(\mathbf{z}_i) - \mathbf{t}_i\|^2 \right) \quad (13)$$

and $\|\cdot\|^2$ is the error metric in the CIE color space. Other metrics may be used if desired. In practice, it may be necessary and desirable to incorporate constraints on \mathcal{F}_{scan} . Specific constraints will be discussed in Section IX-A.

V. PRINTERS

Printer calibration is difficult due to the nonlinearity of the printing process, and the wide variety of methods used for color printing (e.g., lithography, inkjet, dye sublimation, etc.). Because of these difficulties, printing devices are often calibrated with an LUT and interpolation [22], [26]. In other words, the continuum of values are found by interpolating between points in the LUT.

To produce a profile of a printer, a subset of values spanning the space of allowable control values for the printer is first selected. Denote these device dependent values by \mathbf{c}_k for $1 \leq k \leq M_p$. In the printing process, these values produce a set of reflectance spectra which are denoted by \mathbf{p}_k for $1 \leq k \leq M_p$.

The patches \mathbf{p}_k are measured using a colorimetric device as was performed for the scanner calibration, which provides the values

$$\{\mathbf{t}_k = \mathbf{A}^T \mathbf{L}_v \mathbf{p}_k\} \quad \text{for } 1 \leq k \leq M_p. \quad (14)$$

Again, \mathbf{t}_k could represent any colorimetric or device independent values, not just CIE XYZ.

The problem is then to determine a mapping \mathcal{F}_{print} which is the solution to the optimization problem

$$\mathcal{F}_{print} = \arg \left(\min_{\mathcal{F}} \sum_{i=1}^{M_p} \|\mathcal{F}(\mathbf{c}_i) - \mathbf{t}_i\|^2 \right) \quad (15)$$

where as in the scanner calibration problem, there may be constraints which \mathcal{F}_{print} must satisfy.

VI. GAMUT MAPPING

As discussed, color reproduction devices are limited in the colors that they can reproduce which is defined as the device gamut. Gamut mismatch is a problem which occurs when two devices have different gamuts and it is desired to reproduce an image displayed with one device using the other device. Consider two gamuts $G_{monitor}$ and G_{print} . It is desired to print an image that is displayed on the monitor. Assuming $\mathcal{F}_{monitor}$ is known, we can map from the monitor RGB values to CIE values. Now the problem is to map these CIE values to device dependent values for the printer. The problem is that there may be colors which the monitor can display but the printer cannot print. As mentioned in Section II-C, the mapping \mathcal{D} is used for this purpose. The printer control value for the CIE value \mathbf{t} is given by $\mathcal{F}_{printer}^{-1}(\mathcal{D}(\mathbf{t}))$.

Depending upon the desired effect and the media in use, \mathcal{D} may or may not be the identity operator on the colors within G_{print} . The reason for using a \mathcal{D} that is not the identity operator can be illustrated by an example in which there are smoothly varying regions in the image that are outside the printer gamut. These colors will be gamut-mapped to the same color on the gamut boundary, which will result in abrupt edges in the previously smooth region. To reduce this artifact, a gamut mapping is often used, which compresses all the colors in the image to reduce the colorimetric dynamic range in the image while ensuring that all the colors can be reproduced. For example, all the colors in the image could be moved toward one point such as a mid-gray, until all the colors in the image are within the device gamut. Mathematically, this problem can be posed as

$$\min |\alpha| \quad \forall \mathbf{t}_k \in I \quad (16)$$

such that

$$\hat{\mathbf{t}}_k = \mathbf{t}_k + \alpha \mathcal{J}(\mathbf{t}_o - \mathbf{t}_k) \in G$$

where $\hat{\mathbf{t}}_k$ is the updated tristimulus value, \mathbf{t}_o is the mid-gray color, G is the device gamut, I is the set of color values in the image, and \mathcal{J} is a nonlinearity. Unlike a simple clipping approach in which out-of-gamut colors are mapped to the closest in-gamut color, this method will retain some of the variation in smoothly varying image regions that are beyond the device gamut. Note that the above operation is image dependent.

In practice, gamut mapping is performed in a color space in which the Euclidean distance has a perceptual meaning, e.g. CIE Lab [27]. Other work [28], [29] has noted that a method that maps to the closest (Euclidean distance) in-gamut color in a perceptual color space such as CIE Lab produces color differences which are less acceptable than an algorithm that maintains lightness and the hue angle $h = \arctan(b^*/a^*)$. Note, however, that hue angle as defined with the CIE Lab and CIE Luv color spaces relates poorly with perceptual hue in certain regions of the color space [30]. Other work has noted that maintaining chroma is of greater importance than maintaining lightness [31]. For detailed gamut mapping experiments, the reader is referred to [28], [29], [32], and [33].

VII. ILLUMINATION CORRECTION

As previously mentioned, it may be possible to use an existing profile that was created for a particular viewing illuminant along with simple transformations to obtain profiles for other illuminations. The problem can be defined as follows. Let the profile for illuminant \mathbf{L}_v to be given by the mappings \mathcal{F}_{device} , $\mathcal{F}_{device}^{-1}$, and \mathcal{D} , which implies

$$\mathcal{F}_{device}(\mathbf{c}) = \mathbf{t}_{\mathbf{L}_v} = \mathbf{A}^T \mathbf{L}_v \mathbf{r}. \quad (17)$$

If the illuminant for which a new profile is desired is given by \mathbf{L}_{v_2} then the problem is to find an invertible mapping \mathcal{C} such that

$$\mathcal{C}_{illum} = \arg(\min_{\mathcal{C}} E\{\|\mathcal{C}(\mathbf{t}_{\mathbf{L}_v}) - \mathbf{A}^T \mathbf{L}_{v_2} \mathbf{r}\|^2\}). \quad (18)$$

This is a problem in illumination correction which has been studied [34]. Simple matrix transformations will often give acceptable results due to the limited number of colors that are used in the printing process [35]. Once the mapping \mathcal{C} has been determined, the new profile is given by $\mathcal{C}(\mathcal{F}_{device}(\cdot))$, $\mathcal{F}_{device}^{-1}(\mathcal{C}^{-1}(\cdot))$, and \mathcal{D} .

VIII. DIGITAL CAMERAS

The calibration of a digital camera can be formulated in the same manner as that of a scanner with the additional problem of a variable recording illuminant. Unfortunately, the illumination under which an image is recorded can vary among daylight, tungsten, fluorescent, with flash, without flash, etc. Another problem is that the class of reflectance spectra cannot be readily limited for the camera as they can for the desktop scanner. For example, the desktop scanner can be easily calibrated for a particular film/paper type, but the digital camera will be used for recording images with a more varied selection of reflectance spectra.

As mentioned, a profile is typically created for one viewing illuminant. While the images that are printed (or displayed on the monitor) using data from the camera may be viewed under a single illuminant, the recording illuminant is varying for the digital camera from image to image. The problem can be posed as one of determining how to alter the existing profile for the camera based on the illumination under which the image was recorded. To perform this operation, it is necessary to determine the illumination under which the image was recorded [36]–[39]. Once an estimate of the illumination is determined, the problem of correcting for the recording illumination can be approached (cf. Section VII). This problem can be described as follows.

Let there exist a profile \mathcal{F}_{camera} for the digital camera for images recorded under illuminant \mathbf{L}_v (which is also the viewing illuminant for the final images). Due to limited control, an image is recorded under illuminant \mathbf{L}_r giving recorded values of

$$\mathbf{c}_i = \mathbf{N}^T \mathbf{L}_r \mathbf{r}_i \quad (19)$$

at pixels $i = 1, \dots, M$, where the columns of \mathbf{N} are the spectral sensitivity of the camera.

The profile was created for images recorded as

$$\mathbf{d}_i = \mathbf{N}^T \mathbf{L}_v \mathbf{r}_i. \quad (20)$$

The question is what (if any) transformation should be performed on the values \mathbf{c}_i prior to using the mapping \mathcal{F}_{camera} ? For example, if no transformation is performed and \mathbf{L}_v is D50, while \mathbf{L}_r is F2 fluorescent, then the images will appear to have a green cast when later viewed. This effect implies that an illumination correction on the values \mathbf{c}_i is needed. In a manner similar to that in Section VII, the goal is to find a mapping \mathcal{B} such that

$$\mathcal{B}_{illum} = \arg(\min_{\mathcal{B}} E\{\|\mathcal{B}(\mathbf{c}_i) - \mathbf{N}^T \mathbf{L}_v \mathbf{r}_i\|^2\}). \quad (21)$$

In this problem, the variability of \mathbf{r} may not be as readily used as in the correction of illumination for viewing printed samples (cf. Section VII) since the digital camera can also record emissive sources. Once a mapping is determined, the profile for the camera under illuminant \mathbf{L}_r can be expressed as $\mathcal{F}_{camera}(\mathcal{B}(\cdot))$.

IX. IMPLEMENTATION CONSIDERATIONS

A. Constraints

The formulation for the scanner calibration and the printer calibration are mathematically similar. In many practical cases, there are constraints which the mappings should satisfy. For example, in the printer profile there are several practical factors such as ink limit and undercolor removal (discussed below) that often come into play. These are physical constraints which must be considered when constructing LUT's to map between the printer device control values and a CIE color space.

In the case of a printer profile, constraint sets of interest include the following.

- *Data consistency:*

$$\mathcal{F}_{print} \in \{\mathcal{G} \mid \|\mathcal{G}(\mathbf{c}_i) - \mathbf{t}_i\| \leq \delta_v \ i = 1, \dots, M_p\} \quad (22)$$

where δ_v is a just-noticeable-difference (JND) threshold.

- *Inklimit:*

$$\mathcal{F}_{print} \in \{\mathcal{G} \mid \|\mathcal{G}^{-1}(\mathbf{t})\| \leq \delta_{ink} \ \forall \mathbf{t} \in G\} \quad (23)$$

where δ_{ink} is the maximum amount of ink that should be placed on the paper.

- *Smoothness:*

$$\mathcal{F}_{print} \in \{\mathcal{G} \mid \|(\nabla \mathcal{G})(\mathbf{c})\| \leq \delta_{smooth} \ \forall \mathbf{c} \in \Omega_{print}\} \quad (24)$$

where $\nabla \mathcal{G}$ is the gradient of the function \mathcal{G} and Ω_{print} is the range of control values for the printer. The motivation for requiring smoothness is that the underlying physical reproduction process of the printer is usually well behaved (if not then creating a mapping can be difficult) and the solution should be regularized to keep from fitting any noise introduced from the measurement process or from printer variability.

In CMYK printers, undercolor removal is a technique in which the cyan, magenta, and yellow ink amounts are reduced and black ink is added. Typically, the allowable CMYK values are restricted since different CMYK combinations could give rise to the same CIE XYZ value. This restriction is defined by a set H which is itself defined by four curves which map

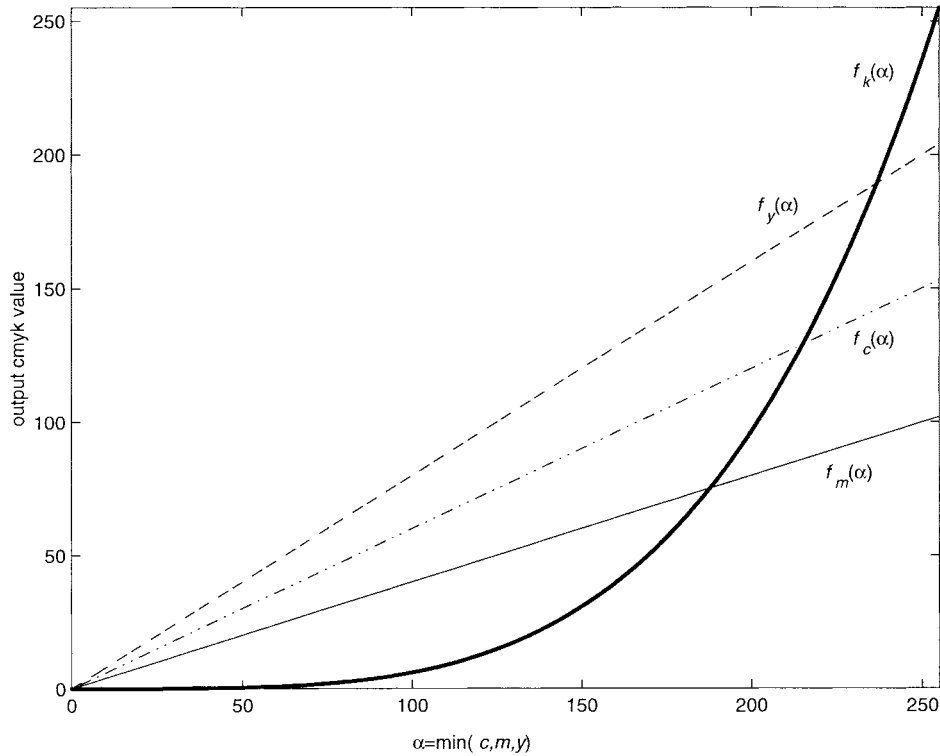


Fig. 1. Undercolor removal curves.

values from $[cmy]$ three-space into $[c'm'y'k']$ four-space. For example, H could be defined as

$$H = \{[c + g_c(\alpha), m + g_m(\alpha), y + g_y(\alpha), f_k(\alpha)] \mid \alpha = \min(c, m, y)\} \quad (25)$$

where $c, m, y \in [0, 255]$, $g_i(\alpha) = f_i(\alpha) - \alpha$, and the curves $f_i(\alpha)$, for $i = (c, m, y, k)$ are as shown in Fig. 1. With H defined, the constraint of undercolor removal is given by

$$\mathcal{F}_{print} \in \{\mathcal{G} \mid \mathcal{G}^{-1}(\mathbf{t}) \in H \forall \mathbf{t} \in G, \} \quad (26)$$

In the LUT based profile, the gamut mapping is implicit in the function which maps from the CIE color space to the device dependent values. In constructing the LUT, gamut-mapping considerations can be incorporated as constraints on the LUT entries. For example, it may be desired that certain points outside the gamut in the LUT provide maximum colorant on the paper (e.g., 100% cyan, 0% yellow, 0% magenta, 0% black). At the same time, one would like to have a smooth transition to the in-gamut colors, and a colorimetrically meaningful way to assign the out-of-gamut colors. Also, recall that the gamut mapping algorithm may operate on the in-gamut colors to maintain the color variation in the image and smoothness of the mapping. Note that incorporating the gamut mapping into the LUT will force gamut mapping to be image independent which may be limiting for certain applications.

Constraints of interest in determining the function \mathcal{D}_{gamut} include the following.

- *Minimum color error:*

$$\mathcal{D}_{gamut} \in \{\mathcal{G} \mid \mathcal{G}(\mathbf{t}) \in G \mathcal{G} = \arg(\min_{\mathcal{K}} \|\mathcal{P}(\mathcal{K}(\mathbf{t})) - \mathcal{P}(\mathbf{t})\|^2) \forall \mathbf{t} \in \Omega_{CIE}\} \quad (27)$$

where \mathcal{P} is a mapping from the CIE color space to a space which is perceptually optimal for gamut mapping (e.g., constant hue and lightness) [29], [40], and \mathcal{K} is in the set of all CIEXYZ to CIEXYZ mappings.

- *Smoothness:*

$$\mathcal{D}_{gamut} \in \{\mathcal{G} \mid \|(\nabla \mathcal{G})(\mathbf{t})\| \leq \delta \forall \mathbf{t} \in \Omega_{CIE}\} \quad (28)$$

- *Fixed points:*

$$\mathcal{D}_{gamut} \in \{\mathcal{G} \mid \mathcal{G}(\mathbf{t}_i) = \mathbf{s}_i \ i = 1, \dots, P\} \quad (29)$$

where there are P fixed points, $\{\mathbf{t}_i\}, \{\mathbf{s}_i\} \ i = 1, \dots, P$, which need to be mapped exactly. Note that common fixed points include paper white being mapped to CIELab [100,0,0] and maximum ink being mapped to CIELab [0,0,0].

Scanner calibration can also be formulated in this framework. The primary sets of interest include the following.

- *Data consistency:*

$$\mathcal{F}_{scan} \in \{\mathcal{G} \mid \|\mathcal{G}(\mathbf{u}_i) - \mathbf{t}_i\| \leq \delta_v \ i = 1, \dots, M_p\} \quad (30)$$

- *Smoothness:*

$$\mathcal{F}_{scan} \in \{\mathcal{G} \mid \|(\nabla \mathcal{G})(\mathbf{u})\| \leq \delta_{smooth} \ \forall \mathbf{u} \in \Omega_{scan}\} \quad (31)$$

where Ω_{scan} is the range of numerical values produced by the scanner, and $\nabla \mathcal{G}$ is the gradient of the function \mathcal{G} .

B. Color Perception

Color is a psychovisual phenomena and is subject to extensive processing by the visual cortex. The appearance of a color stimulus is affected by changes in illumination, surrounding colors, etc. In practice, it is necessary to consider these effects when constructing profiles. For example, a CIE Lab value of $[100, 0, 0]$, which is usually the white point in a profile, should be mapped to the white point of a monitor and the white point of the printer even if neither the paper or monitor white have a CIE Lab value of $[100, 0, 0]$. If this mapping is not performed, then the printed image may have an undesired color cast compared to the monitor, or vice versa.

Color perception can be included into the construction of the profile by performing the transformation to the perceptual color space on the measurements from the samples which are used for the construction of the profile. Typically, a perceptual color space accounts for white point adaptation, color constancy, and other viewing conditions. As before, the patches \mathbf{p}_k are measured using a colorimetric device giving

$$\{\mathbf{t}_k = \mathbf{A}^T \mathbf{L}_v \mathbf{p}_k\} \quad \text{for } 1 \leq k \leq M_p. \quad (32)$$

These values are then mapped to the values $\mathbf{v} = \mathcal{M}(\mathbf{t})$ where \mathcal{M} maps the CIE values to a perceptual color space such as those found in [41]–[43]. The profile LUT is then constructed between the values $\{\mathbf{v}_k = \mathcal{M}(\mathbf{t}_k)\}$ and the device control values \mathbf{c}_k .

As an example, consider the monitor calibration problem. There is no “viewing illuminant” for the monitor, but if visual matches are desired with prints that are viewed under various illuminations, it is necessary to alter the CIE XYZ values used for the mapping between monitor control values and the CIE device independent space to account for the different viewing illuminations.

One simple approach is for the mapping \mathcal{M} to scale the CIE XYZ values such that maximum white is mapped to the white point of the viewing illuminant. Such a process is called *white point mapping*, and the reasoning behind it is that the white point is used as a reference by the HVS. Specifically the mapping could be defined by

$$\mathcal{M}(\mathbf{t}) = \begin{bmatrix} M_X & 0 & 0 \\ 0 & M_Y & 0 \\ 0 & 0 & M_Z \end{bmatrix} \begin{bmatrix} t_1 \\ t_2 \\ t_3 \end{bmatrix} \quad (33)$$

where

$$[M_X, M_Y, M_Z] = \left[\frac{g_1}{W_X}, \frac{g_2}{W_Y}, \frac{g_3}{W_Z} \right]$$

$$\begin{bmatrix} W_X \\ W_Y \\ W_Z \end{bmatrix} = \begin{bmatrix} X_{R \max} & X_{G \max} & X_{B \max} \\ Y_{R \max} & Y_{G \max} & Y_{B \max} \\ Z_{R \max} & Z_{G \max} & Z_{B \max} \end{bmatrix} \begin{bmatrix} 1 \\ 1 \\ 1 \end{bmatrix}$$

$$\mathbf{g} = \beta \mathbf{A}^T \mathbf{l}_v.$$

\mathbf{l}_v is the viewing illumination written as a vector and β is selected so that $\mathbf{g} = [g_1, g_2, g_3]$ is within the gamut of the monitor.

C. LUT Construction

For the construction of a profile LUT, there are two primary approaches. The main difference between the two approaches is the number of sample measurements required. One approach uses a model (e.g. colorimetric or spectral Neugabauer for a printer [44]–[47]) to provide a functional mapping from the device control values to CIE colorimetric values. The model parameters, are determined by collecting a few measurements. This functional mapping can be used to generate a LUT, which is inverted and used to print specified in-gamut CIE values. Unfortunately, there is no one printer model that works well for the large variety of printing processes.

Another approach relies on a very large sampling of the device control values, such that LUT entries can be determined via interpolation and extrapolation from the measured values. The advantage of this approach is that no physical model is required. The disadvantages of the model-free approach are that collecting the large number of measurements can be time consuming, and it is difficult to know how to update the LUT if a minor change in printing conditions occurs (e.g., paper lot or ink lot changes).

X. EXAMPLES

To demonstrate artifacts from gamut mapping and the effect from gamut mismatch, an RGB image was created on a monitor. The image, shown in Fig. 2(a), consists of two figures. One figure is a color wheel which displays a continuum of RGB values such that one of the values is always zero (e.g., $RGB = [0 \ 240 \ 120]$). The other figure is a series of color bars each of which smoothly step from black, to a primary color (e.g. red, green, blue, cyan, magenta, yellow), and then to white. For example, the red bar was created by stepping through the RGB vector sequence $\{[0 \ 0 \ 0], [1 \ 0 \ 0], \dots, [255 \ 0 \ 0], [255 \ 1 \ 1], \dots, [255 \ 255 \ 255]\}$. The smooth transitions between highly saturated colors make these figures ideal for demonstrating gamut mapping artifacts.

A monitor profile was created between the monitor RGB values and CIE Lab D50 (i.e. $\mathcal{F}_{monitor}$ was created) via the procedure described in Section III. A dye sublimation (dye-sub) [48] RGB printer (three-color CMY printer which accepted RGB input values) was also profiled for CIE Lab D50 (i.e. \mathcal{F}_{print}^{-1} was created) to printer RGB space. As discussed in Section V, this profile was created by measuring a series of color patches with a colorimeter and creating an LUT. Out of gamut colors were mapped, via \mathcal{D} , to the closest in gamut value, along a constant hue angle while preserving lightness in CIE Lab space. Three different images were printed and are shown in Fig. 2. The images are as follows:

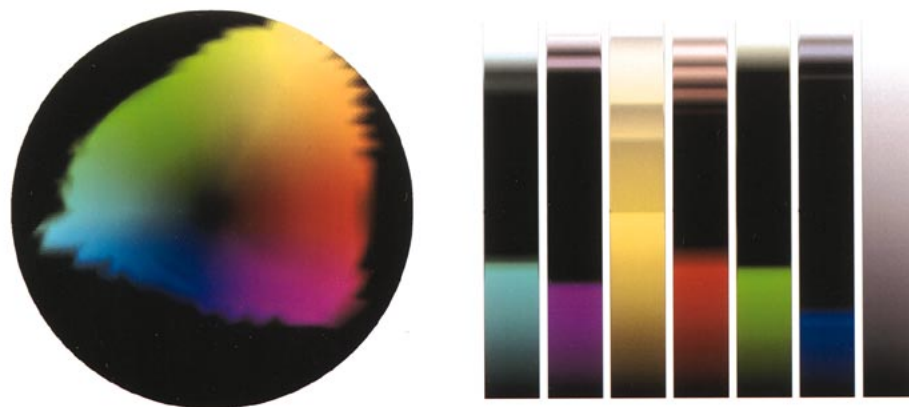
- a) image created by sending monitor RGB values, \mathbf{m}_k (\mathbf{m}_k is the k th pixel RGB value for the image), directly to the printer with no processing;
- b) image created by sending the values $\mathcal{F}_{print}^{-1}(\mathcal{D}(\mathcal{F}_{monitor}(\mathbf{m}_k)))$ to the printer;
- c) Image created by sending the values $\mathcal{F}_{print}^{-1}(\mathcal{U}(\mathcal{F}_{monitor}(\mathbf{m}_k)))$ to the printer, where \mathcal{U} maps colors outside of the printer gamut to black and is the identity operator on the in-gamut colors.



(a)



(b)



(c)

Fig. 2. Artificial images. (a) Unprocessed image. (b) Corrected image. (c) Out-of-gamut values mapped to black.

As can be seen in Fig. 2(c), there are a significant number of colors outside of the printer gamut. In the bar figure of Fig. 2(c), the banding (especially in the yellow bar) indicates that the values are going in and out of the printer gamut as the monitor device dependent control values are stepped from black to a primary color and then to white. In addition, blocking artifacts are visible in Fig. 2(b) where previously

smoothly varying regions [as shown in Fig. 2(a)] are mapped to the same area on the gamut boundary. Note also that the monitor pure red does not map to a pure red on the printer. This is often an issue in gamut mapping, and suggests the need for the use of a constraint such as that given in (29).

To demonstrate the need for improved color management, an original (i.e., printed) version of the Lena image was scanned

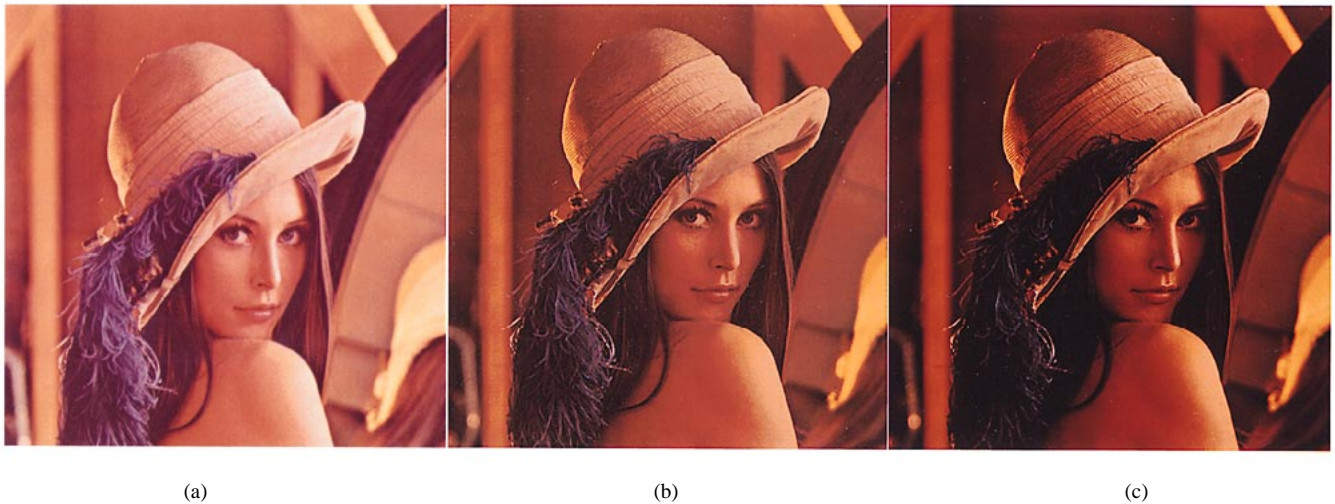


Fig. 3. Lena Images. (a) Commonly used image. (b) Corrected image. (c) Unprocessed scan.

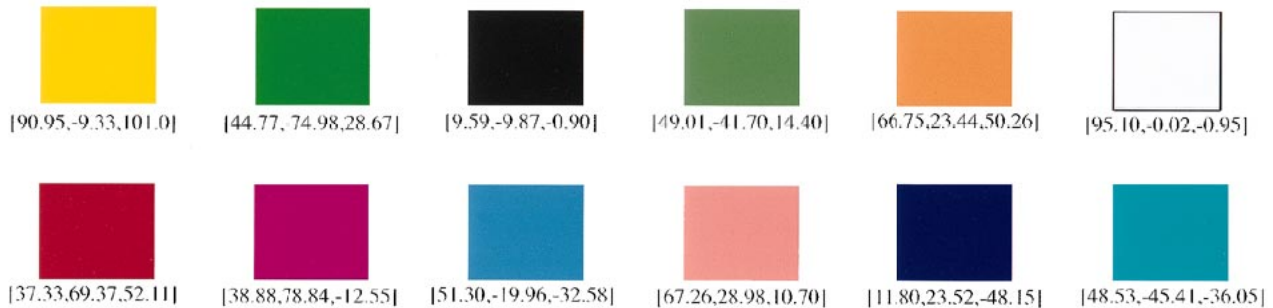


Fig. 4. Color squares and their CIELab values for assessing color reproduction accuracy of this issue.

on a desktop scanner. The scanned image will be referred to as the newly scanned Lena image. In addition, a color target was scanned which contained 276 color patches. The target patches were measured with a colorimeter and a LUT mapping was determined from scanned RGB values to CIELab D50 (i.e. \mathcal{F}_{scan} was created). For comparison, the commonly used digital color Lena image was obtained. This will be referred to as the standard Lena image.

The LUT for the dye-sub printer that was used for Example 1 was used to map from the CIELab D50 values to printer control values. Three images were printed and are shown in Fig. 3 for comparison. The images are as follows where \mathbf{l}_k is the k th pixel RGB value for the standard Lena image and \mathbf{ls}_k is the k th pixel RGB value for the newly scanned Lena image:

- image created by sending the RGB values \mathbf{l}_k directly to the printer with no processing;
- image created by sending the values $\mathcal{F}_{print}^{-1}(\mathcal{D}(\mathcal{F}_{scan}(\mathbf{ls}_k)))$ to the printer;
- image created by sending the values \mathbf{ls}_k directly to the printer with no processing.

It is worthwhile to compare the Lena images in Fig. 3 with the images printed in the special issue of the TRANSACTIONS July 1997 [49, p. 960].

Fig. 3(a) closely matches those in the special issue, while Fig. 3(b) is a close match to the original printed image (unavailable to most readers). Simply providing the scanned

RGB values directly to the printer produces a much different image as shown in Fig. 3(c). One should realize, however, that the commonly displayed Lena image is just that, a scanned RGB image which is often provided directly as input to the available color printer. Comparison of Fig. 3(a) and (c) gives an indication of the differences in the raw scanner data. The large differences between Fig. 3(a) and (c) demonstrate that widely different results can occur depending upon how an image is scanned, processed, and printed. This is a significant problem when attempting to convey the results of a color image processing algorithm, and to compare those results with previously archived material. Finally, note that in Fig. 3(b) the shoulder and arm region of Lena contains minor blocking artifacts due to gamut mapping problems.

In the publication process, the color images in this paper are further processed, which will introduce artifacts and loss of accuracy (due to lack of control, gamut differences, etc). To quantify this effect, we have provided an additional image containing color squares in Fig. 4. The CIELab D50 values are given for each square on the original dye-sub print. Readers are encouraged to measure the color squares to test the reproduction accuracy of the process if they have access to a colorimeter. If not, the measured values after publication are available at <ftp://ftp.eos.ncsu.edu/pub/hjt/profile>. All images produced in these examples, data used to create the profiles, and the profiles are also available at this location.

XI. CONCLUSIONS

The problem of achieving color management by calibrating scanners, monitors, and printers was defined mathematically. This lays a framework upon which sophisticated color image processing methods may be developed. The ease with which the constraint sets are formulated, as shown in Section IX-A, demonstrates the usefulness of the framework. The importance of the problem was made clear by consideration of the vast differences in appearance between images produced by calibrated and uncalibrated systems. This more formal approach of producing calibrated color output should become standard procedure when displaying images for the image processing community.

There still exist many open and interesting problems in color recording and reproduction. Many of these problems are well suited for a signal processing approach. For example, with the advent of high-fidelity six color printing processes, the higher dimensionality of the mapping becomes a problem. With the use of multiple inks, these printers also introduce an interesting problem in the determination of transformations which minimize certain criteria such as cost of ink, total ink, etc.

Printing processes change over time due to environmental factors (e.g., temperature, humidity, etc.) and due to dye changes, paper changes, etc. Performing a complete calibration can be very time consuming. It is of great interest to quickly update an existing calibration. Likely approaches include adaptive filtering, neural nets, and partial sampling. Of course, it is always profitable to reduce the number of measurements required for a complete calibration while maintaining accuracy.

The problem of gamut mapping is far from optimally solved. In fact, there is such a variety of devices that each one presents its own unique set of problems. The ideal gamut mapping depends upon the image, the source gamut size, and the destination gamut size. The viewing intent and preferences of the user play a critical role in determining what is optimal. Thus, there does not appear to be a global solution to such problems.

The nonuniformity of CIELab in the blue/magenta region causes problems with gamut mapping algorithms that use constant hue mapping in this space. Furthermore, the CIE metrics are based upon matching patches of color, not the overall appearance of images. Image-based metrics are an open research area, although not a true signal processing problem. However, as new error metrics are developed, it is of interest to incorporate these into the device profiling methods.

Color image reproduction and recording technology is moving at a rapid pace. The advent of these new instruments provides research opportunities to create accurate color with these instruments. Color filter arrays and multispectral recording are new input modalities that require investigation. The eminent introduction of new display technologies, such as flat panels of various types and micromirror devices, makes understanding basic calibration requirements very important to achieving the optimal performance from these devices. In addition, the design of the instruments presents several problems requiring signal processing methods. Examples include

the determination of optimal monitor phosphors, optimal inks for printing, and optimal scanning filters for recording images that will be reproduced on specific output devices.

Finally, with the growth of the world wide web and e-commerce, the transmission of accurate color over the network is of interest. In particular, while coding is currently an active research area, there is need to determine the optimal representations and auxiliary information, e.g., viewing illuminant, primary colorant for reconstruction, etc., are required for accurate reproduction. The effect of various types of errors in the transmission of color images will affect the profile data that needs to be included with the image data.

REFERENCES

- [1] H. J. Trussell *et al.*, Eds., *IEEE Trans. Image Processing, Spec. Issue Color Imag.*, vol. 6, July 1997.
- [2] J. B. Cohen, "Color and color mixture: Scalar and Vector fundamentals," *Color Res. Appl.*, vol. 13, pp. 5–39, Feb. 1988.
- [3] B. A. Wandell, "The synthesis and analysis of color images," *IEEE Trans. Pattern Anal. Machine Intell.*, vol. PAMI-9, pp. 2–13, Jan. 1987.
- [4] H. J. Trussell and J. R. Sullivan, "A vector-space approach to color imaging systems," *Proc. SPIE: Image Processing Algorithms and Techniques*, K. S. Pennington, Ed., vol. 1244, pp. 264–271, 1990.
- [5] H. J. Trussell, "Application of set theoretic models to color systems," *Color Res. Appl.*, vol. 16, pp. 31–41, Feb. 1991.
- [6] R. L. Alfvén and M. D. Fairchild, "Observer variability in metameric color matches using color reproduction media," *Color Res. Appl.*, vol. 22, pp. 174–188, June 1997.
- [7] Int. Color Consort., "Int. color consort. profile format Ver. 3.4," available at <http://color.org/>.
- [8] G. B. Pawle, "Inside the ICC color device profile," in *Proc. IS&T/SID 3rd Color Imag. Conf.: Color Sci., Syst., Appl.*, Scottsdale, AZ, Nov. 7–10, 1995, pp. 160–163.
- [9] W. B. Cowan, "An inexpensive scheme for calibration of a color monitor in terms of standard CIE coordinates," *Comput. Graph.*, vol. 17, pp. 315–321, July 1983.
- [10] R. S. Berns, R. J. Motta, and M. E. Grozynski, "CRT Colorimetry. Part I: Theory and practice," *Color Res. Appl.*, vol. 18, pp. 5–39, Feb. 1988.
- [11] ———, "CRT Colorimetry. Part II: Metrology," *Color Res. Appl.*, vol. 18, pp. 315–325, Feb. 1988.
- [12] V. Mani, "Calibration of color monitors," M.S. thesis, North Carolina State Univ., Raleigh, 1991.
- [13] G. Sharma and H. J. Trussell, "Figures of merit for color scanners," *IEEE Trans. Image Processing*, vol. 6, pp. 990–1001, July 1997.
- [14] P. Vora and H. J. Trussell, "Mathematical methods for the analysis of color scanning filters," *IEEE Trans. Image Processing*, vol. 6, pp. 312–320, Feb. 1997.
- [15] G. Sharma, H. J. Trussell, and M. J. Vrhel, "Optimal nonnegative color scanning filters," *IEEE Trans. Image Processing*, vol. 7, pp. 129–133, Jan. 1998.
- [16] M. J. Vrhel and H. J. Trussell, "Optimal color filters in the presence of noise," *IEEE Trans. Image Processing*, vol. 4, pp. 814–823, June 1995.
- [17] M. Wolski, J. P. Allebach, C. A. Bouman, and E. Walowitz, "Optimization of sensor response functions for colorimetry of reflective and emissive objects," *IEEE Trans. Image Processing*, vol. 5, pp. 507–517, Mar. 1996.
- [18] J. B. Cohen, "Dependency of the spectral reflectance curves of the munsell color chips," *Psychonom. Sci.*, vol. 1, pp. 369–370, 1964.
- [19] J. Ho, B. Funt, and M. S. Drew, "Separating a color signal into illumination and surface reflectance components: theory and applications," *IEEE Trans. Pattern Anal. Machine Intell.*, vol. 12, pp. 966–977, Oct. 1990.
- [20] M. J. Vrhel, R. Gershon, and L. S. Iwan, "Measurement and analysis of object reflectance spectra," *Color Res. Appl.*, vol. 19, pp. 4–9, Feb. 1994.
- [21] B. K. P. Horn, "Exact reproduction of colored images," *Comput. Vis., Graph., Image Process.*, vol. 26, pp. 135–167, 1984.
- [22] P. C. Hung, "Colorimetric calibration in electronic imaging devices using a look-up table model and interpolations," *J. Electron. Imag.*, vol. 2, pp. 53–61, Jan. 1993.
- [23] H. R. Kang and P. G. Anderson, "Neural network applications to the color scanner and printer calibrations," *J. Electron. Imag.*, vol. 1, pp. 125–134, Apr. 1992.
- [24] H. Haneishi, T. Hirao, A. Shimazu, and Y. Mikaye, "Colorimetric precision in scanner calibration using matrices," in *Proc. 3rd IS&T/SID*

- Color Imaging Conf.: Color Science, Systems and Applications*, Nov. 1995, pp. 106–108.
- [25] H. R. Kang, "Color scanner calibration," *J. Imag. Sci. Technol.*, vol. 36, pp. 162–170, Mar./Apr. 1992.
- [26] J. Z. Chang, J. P. Allebach, and C. A. Bouman, "Sequential linear interpolation of multidimensional functions," *IEEE Trans. Image Processing*, vol. 6, pp. 1231–1245, Sept. 1997.
- [27] L. W. MacDonald, "Gamut mapping in perceptual color space," in *Proc. IS&T/SID's 3rd Color Imaging Conf.: Transforms and Transportability of Color*, Nov. 1993, pp. 193–196.
- [28] T. Hoshino and R. S. Berns, "Color gamut mapping techniques for color hard copy images," in *Proc. SPIE*, vol. 1990, pp. 152–165, 1993.
- [29] F. Ebner and M. D. Fairchild, "Gamut mapping from below: Finding minimum perceptual distances for colors outside the gamut volume," *Color Res. Appl.*, vol. 22, pp. 402–413, Dec. 1997.
- [30] P. Hung and R. S. Berns, "Determination of constant hue loci for a CRT gamut and their predictions using color appearance spaces," *Color Res. Appl.*, vol. 20, pp. 285–295, Oct. 1997.
- [31] J. Morovic and M. R. Luo, "Gamut mapping algorithms based on psychophysical experiment," in *Proc. IS&T/SID 5th Color Imaging Conf.: Color Science, Systems and Applications*, pp. 44–49, 1997.
- [32] E. D. Montag and M. D. Fairchild, "Psychophysical evaluation of gamut mapping techniques using simple rendered images and artificial gamut boundaries," *IEEE Trans. Image Processing*, vol. 6, pp. 977–989, July 1997.
- [33] J. Morovic and M. R. Luo, "Cross-media psychophysical evaluation of gamut mapping algorithms," in *Proc. AIC Color '97*.
- [34] M. J. Vrhel and H. J. Trussell, "Color correction using principal components," *Color Res. Appl.*, vol. 17, pp. 328–338, Oct. 1992.
- [35] ———, "Physical device illumination color correction," *SPIE Proc.: Device-Independent Color Imaging and Imaging Systems Integration*, vol. 1909, pp. 84–91, Aug. 1993.
- [36] K. R. L. Godfrey and Y. Attikiouzel, "Polar backpropagation—Determining the chromaticity of a light source," in *Int. Neural Network Conf.*, Paris, France, July 9–13, 1990.
- [37] H. C. Lee, "Method for computing the scene-illuminant chromaticity from specular highlights," *J. Opt. Soc. Amer. A*, vol. 3, pp. 1694–1699, Oct. 1986.
- [38] C. F. Borges, "Trichromatic approximation method for surface illumination," *J. Opt. Soc. Amer. A*, vol. 8, pp. 1319–1325, 1991.
- [39] H. J. Trussell and M. J. Vrhel, "Estimation of illumination for color correction," in *Proc. IEEE ICASSP '91*, vol. 4, pp. 2513–2516.
- [40] N. Katoh and M. Ito, "Gamut mappings for computer generated images (II)," in *Proc. IS&T/SID 4th Color Imaging Conf.: Color Science, Systems, and Applications*, pp. 126–129, 1996.
- [41] R. W. G. Hunt, "Revised color-appearance model for related and unrelated colors," *Color Res. Appl.*, vol. 16, pp. 146–165, June 1991.
- [42] M. D. Fairchild, "Refinement of the RLAB color space," *Color Res. Appl.*, vol. 21, pp. 338–346, Oct. 1996.
- [43] Y. Nayatani *et al.*, "Comparison of color-appearance models," *Color Res. Appl.*, vol. 15, pp. 272–284, Oct. 1990.
- [44] H. E. J. Neugebauer, "Die theoretischen Grundlagen des Mehrfarbenbuchdrucks," *Zeitschrift wissenschaft. Photogr. Photochem.*, vol. 36, pp. 73–89, Apr. 1937, reprinted in [47].
- [45] J. A. S. Viggiano, "Modeling the color of multi-colored halftones," in *Proc. TAGA*, pp. 44–62, 1990.
- [46] R. Balasubramanian, "Colorimetric modeling of binary color printers," in *Proc. IEEE ICIP*, Nov. 1995, vol. 2, pp. 327–330.
- [47] K. Sayangi, Ed., *Proc. SPIE: Neugebauer Memorial Seminar on Color Reproduction*, vol. 1184, Dec. 1989.
- [48] R. A. Hann and N. C. Beck, "Dye diffusion thermal transfer (D2C2) color printing," *J. Imag. Technol.*, vol. 16, pp. 238–241, Dec. 1990.
- [49] J. R. Goldschneider, E. A. Riskin, and P. W. Wong, "Embedded multilevel error diffusion," *IEEE Trans. Image Processing*, vol. 6, pp. 956–964, July 1997.



Michael J. Vrhel (M'93) was born in St. Joseph, MI, in 1964. He received the B.S. degree in electrical engineering from Michigan Technological University, Houghton, in 1987, and the M.S. and Ph.D. degrees in electrical engineering from North Carolina State University, Raleigh, in 1989 and 1993, respectively.

From 1993 to 1996, he was a National Research Council Associate at the National Institutes of Health, Biomedical Engineering and Instrumentation Program. Currently, he is the Senior Scientist at Color Savvy Systems Limited, Springboro, OH. His research interests include color reproduction, signal restoration/reconstruction, and wavelets.



H. Joel Trussell (S'75–M'76–SM'91–F'94) received the B.S. degree from Georgia Institute of Technology, Atlanta, in 1967, the M.S. degree from Florida State University, Tallahassee, in 1968, and the Ph.D. degree from the University of New Mexico, Albuquerque, in 1976.

He joined the Los Alamos Scientific Laboratory, Los Alamos, NM, in 1969, where he began working in image and signal processing in 1971. During 1978–1979, he was a visiting professor at Heriot-Watt University, Edinburgh, U.K., where he worked with both the university and industry on image processing problems. In 1980, he joined the Electrical and Computer Engineering Department, North Carolina State University, Raleigh. From 1988 to 1989, he was a Visiting Scientist at the Eastman Kodak Company, Rochester, NY, and from 1997 to 1998 he was a Visiting Scientist at Color Savvy Systems, Springboro, OH. He has taught a wide variety of subjects in the signal and image processing areas. His research interests include estimation theory, signal and image restoration, accurate measurement, and reproduction of color.

Dr. Trussell is a past associate editor for the TRANSACTIONS ON ACOUSTICS, SPEECH, AND SIGNAL PROCESSING, and is currently an associate editor for the SIGNAL PROCESSING LETTERS. He was a member and past chairman of the Image and Multidimensional Digital Signal Processing Committee of the Signal Processing Society of the IEEE.